Finite-element modelling of 3d oblique ultrasonically assisted turning of TI-6AL-4V

Laurence A. Coles, Anish Roy and Vadim V. Silberschmidt
L.Coles@lboro.ac.uk & A.Roy3@lboro.ac.uk &
V.Silberschmidt@lboro.ac.uk

Abstract

This study outlines the development of a new three-dimensional FE modelling approach used to study the conventional and ultrasonically assisted oblique turning processes of titanium (Ti-6Al-4V) alloy. Numerical simulations with the models demonstrated that for the chosen machining parameters, the ultrasonically assisted turning (UAT) process resulted in a 20% reduction in the tangential cutting force compared to that in the conventional turning (CT) process. The new approach enables the more accurate prediction of the CT and UAT processes, while allowing the complete control of the machining parameters within the 'real-time' turning simulation. This allows for the prediction of the cutting force, resultant and residual stresses and chip formation.

1 Introduction

Hybrid machining processes have gained sufficient prominence in the manufacturing industry. Ultrasonically assisted machining (UAM) is a hybrid machining technique, in which high-frequency, low-amplitude vibration is superimposed on the cutting tool movement, resulting in several well-documented advantages. Recent studies have seen the development of the ultrasonically assisted turning (UAT) process in which the resultant cutting forces show substantial reduction (in some cases >70%), as well as improved surface finish amongst other advantages [1, 2, 3, 4]. The UAM process has shown advantages when applied to the drilling of composite materials [5].

Direct experimental studies of machining processes are expensive and time-consuming, especially when there is a wide range of machining parameters that affect the complex hybrid thermo-mechanical machining process. In recent years, the use of mathematical simulations and, in particular, finite-element (FE) techniques has gained prominence in the research community; from the application of Smooth-Particle Hydrodynamics (SPH) in the turning of metals [6, 7], to the 2D and 3D FE modelling of both the conventional and ultrasonically assisted turning of many advanced alloys [8, 9, 10]. These modelling approaches are typically restricted to simulations of orthogonal machining, which is not a true representation of the actual cutting process, typically referred to as *oblique machining*.

This study is a part of on-going research at the Wolfson School of Mechanical and Manufacturing Engineering, Loughborough University, UK, on multi-scale FE modelling of advanced machining processes. This paper outlines the current progress made on the development of a 'real-time' FE models of both the CT and UAT processes.

2 Finite-element model of turning

A schematic of an oblique turning is shown in Figure 1, with the cutting tool geometry taken from [2]. A FE model of the cutting in CT and UAT is shown in Figure 2 with the cutting parameters listed in Table 2. The modelled domain formed a 5° section of the work piece together with the previous tool path (including the 0.1 mm/rev feed rate off-set). The work piece was fixed with respect to the X-axis (axial direction) and rotated towards the cutting tool. For CT the cutting tool was fixed in the Y (radial) and Z (tangential) directions, with the tool feed rate applied in the X (axial) direction. In UAT, ultrasonic vibration was applied in the Z (tangential) direction as shown in Figure 2. The cutting tool was modelled as a rigid body. This modelling approach allows for the full 3D oblique modelling of the CT and UAT process. This model was develop using the commercial FE software SIMULIA Abaqus/Explicit 6.14.

The workpiece material was Ti-6Al-4V, with it's behaviour described using a nonlinear temperature- and strain-rate-sensitive Johnson-Cook (JC) material model using parameters A, B, n, C, m, T_m along with other parameters as mentioned in [11] and can be found in Table 2.

The primary equation of the JC model is

$$\sigma_y = [A + B(\epsilon_p)^n][1 + C\ln(\dot{\epsilon}_p^*)][1 - (T^*)^m)], \tag{1}$$

where

$$\dot{\epsilon}_p^* = \frac{\dot{\epsilon}_p}{\dot{\epsilon}_{p0}}, \qquad T^* = \frac{(T - T_0)}{(T_m - T_0)}. \tag{2}$$

Here, ϵ_p is the effective plastic strain, $\dot{\epsilon}_p$ and $\dot{\epsilon}_{p0}$ are the plastic strain rate and effective plastic strain rate used for the calibration of the model respectively, T and T_0 are the current and reference temperatures respectively.

The workpiece was discretised with a refined mesh around the cutting process zone. For both CT and UAT models, 686565 linear hexahedral coupled temperature-displacement elements (C3D8RT) were used. The cutting tool was meshed using quadratic tetrahedral elements (C3D10M). Contact between the cutting tool and the workpiece was defined as a hard contact for its normal behaviour, with a coefficient of friction of 0.3384 [12] along with a shear stress limit.

Given the large deformations observed within the cutting process zone, arbitrary lagrangian eulerian (ALE) re-meshing was employed to allow for increased plastic flow of the material and formation of the chip. ALE re-meshing parameters were

calibrated based on the cutting speed and minimum element size. Mass scaling was used to improve computational efficiency for both models. The total modelled machining time was 0.8 ms, which was sufficient for achieving consistent cutting forces.

3 Results and Discussion

The developed fully 3D approach allows the observation of the tangential and axial cutting forces with increased accuracy, the radial forces are still challenging to observe given the discretised nature of the FE method. At this initial stage, the tangential cutting forces (Z direction) were monitored, with the average force observed from the CT model reaching 50.9 N and for UAT 40.3 N. As a result, it can be shown that the additional ultrasonic vibration leads to an approximate 20% reduction of the tangential cutting forces, which is within the range seen in the previous study. It was found with these models that for the defined turning parameters, the UAT peak cutting force was similar to that of CT but the ultrasonic vibration allowed the tool to dis-engage form the workpiece (decreasing the force) before subsequent re-engaging, resulting in the lower average cutting force.

With reference to Figure 3 it can be seen that stress distributions within the local process zone for both the CT and UAT processes are very similar, showing the shear failure region as expected; still, but shows no significant qualitative differences can be observed. Examining the peak stresses in the process zone for each process, it can be seen that the CT process produces a stress of approximately 1730 MPa and the UAT process produces 1577 MPa and 1728 MPa for maximum retraction and penetration of the ultrasonic cycle, respectively. This modelling approach can then also be used to model the residual stresses induced by CT or UAT.

When examining the initial chip formation in both processes, it can been seen that both chips begin to form full 3D helical shape as commonly observed as a result of real oblique turning. Closer examination suggests that the radii of both chips are similar, but without a longer simulated time the true chip formation and length before breakage cannot be assessed properly. Both the CT and UAT models took approximately 48 hours of computational time to run across 12 cores, demonstrating that the approach remains suitably efficient at this initial stage.

4 Conclusions

This paper presents a new modelling approach for simulating both conventional and ultrasonically assisted turning of a titanium alloy. It allows for the complete control of the machining parameters within the simulation, while modelling the 'real-time' turning and workpiece deformation. As a result, this allows for the prediction of the cutting force as well as an assessment of the resultant and residual stresses and chip formation. The following conclusion are made:

1. It can been seen that for the chosen machining parameters the UAT process ofters a 20% reduction in the average tangential cutting force compared to that in the CT process, as expected and found in the literature.

2. This new modelling approach produces a more accurate prediction of the CT and UAT processes taking into account their important 3D cutting geometry which, in turn, enables a greater understanding of the effect of the machining parameters on both processes.

3. The modelling approach shall be developed and taken forward to further investigate and characterisate both processes in more detail, while also make vital comparisons to experimental studies.

5 Acknowledgement

AR and VVS gratefully acknowledges the funding from the Engineering and Physical Sciences Research Council (UK) through grant EP/K028316/1 and Department of Science and Technology (India), project MAST.

References

[1] N. Ahmed, A.V. Mitrofanov, V.I. Babitsky, V.V. Silberschmidt, Analysis of forces in ultrasonically assisted turning. Journal of Sound and Vibration, 2007. 308: p. 845-854.

[2] A. Maurotto, R. Muhammad, A. Roy, V.V. Silberschmidt, Enhanced ultrasonically assisted turning of a β-titanium alloy, Ultrasonics, 2013. 53(7): p. 1242-1250.

[3] R. Muhammad, M.S. Hussain, A. Maurotto, C. Siemers, A. Roy, V.V. Silberschmidt, Analysis of a free machining $\alpha + \beta$ titanium alloy using conventional and ultrasonically assisted turning, Journal of Materials Processing Technology, 2014. 214(4): p. 906-915.

[4] R. Muhammad, A. Maurotto, M. Demiral, A. Roy, V.V. Silberschmidt, Thermally enhanced ultrasonically assisted machining of Ti alloy, CIRP Journal of Manufacturing Science and Technology, 2014. 7(2): p. 159-167.

[5] F. Makhdum, V. A. Phadnis, A. Roy, V. V. Silberschmidt, Effect of ultrasonically-assisted drilling on carbon-fibre-reinforced plastics, Journal of Sound and Vibration, 2014. 333(23): p. 5939-5952.

[6] A. Zahedi, S. Li, A. Roy, V. Babitsky, V. V. Silberschmidt, Application of Smooth-Particle Hydrodynamics in metal machining, Journal of Physics: Conference Series, 2012. 382(1): 012017

[7] A. Zahedi, M. Demiral, A. Roy, V. V. Silberschmidt, FE/SPH modelling of orthogonal micro-machining of f.c.c. single crystal, Computational Materials Science, 2013. 78: p. 104-109.

[8] A.V. Mitrofanov, V.I., Babitsky, V.V. Silberschmidt, Thermomechanical finite element simulations of ultrasonically assisted turning. Computational Materials Science, 2005. 32: p. 463-471.

[9] N. Ahmed, A.V., Mitrofanov, V.I. Babitsky, V.V. Silberschmidt, 3D finite element analysis of ultrasonically assisted turning. Computational Materials Science, 2007. 39: p. 149-154.

[10] R. Muhammad, N. Ahmed, A. Roy, V.V. Silberschmidt, Numerical modelling of vibration-assisted turning of Ti-15333. Procedia CIRP, 2012. 1(0): p. 347-352.

[11] X. Wang, J. Shi, Validation of Johnson-Cook plasticity and damage model using impact experiment, International Journal of Impact Engineering, 2013. 60: p. 67-75.

[12] D. Smolenicki, J. Boos, F. Kuster, H. Roelofs, C.F. Wyen, In-process measurement of friction coefficient in orthogonal cutting, CIRP Annals - Manufacturing Technology, 2014. 63: p. 97-100

Laurence A. Coles, Anish Roy and Vadim V. Silberschmidt, Loughborough University, Wolfson School of Mechanical and Manufacturing Engineering, Loughborough University, Leicestershire, LE11 3TU, UK

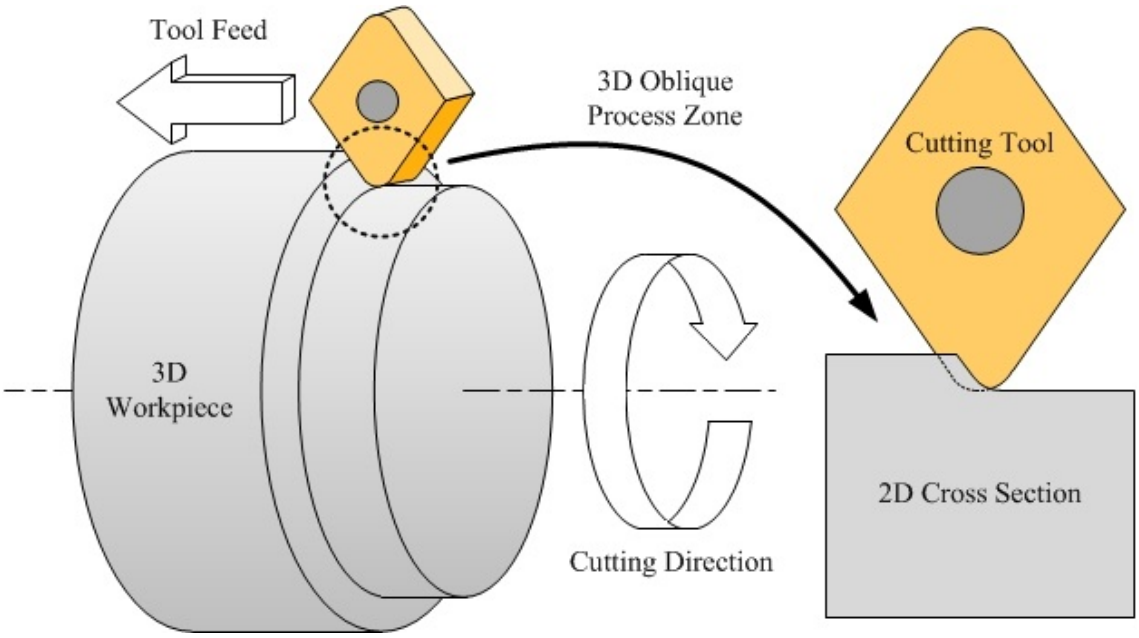

Figure 1: True 3D oblique curved cutting path turning process

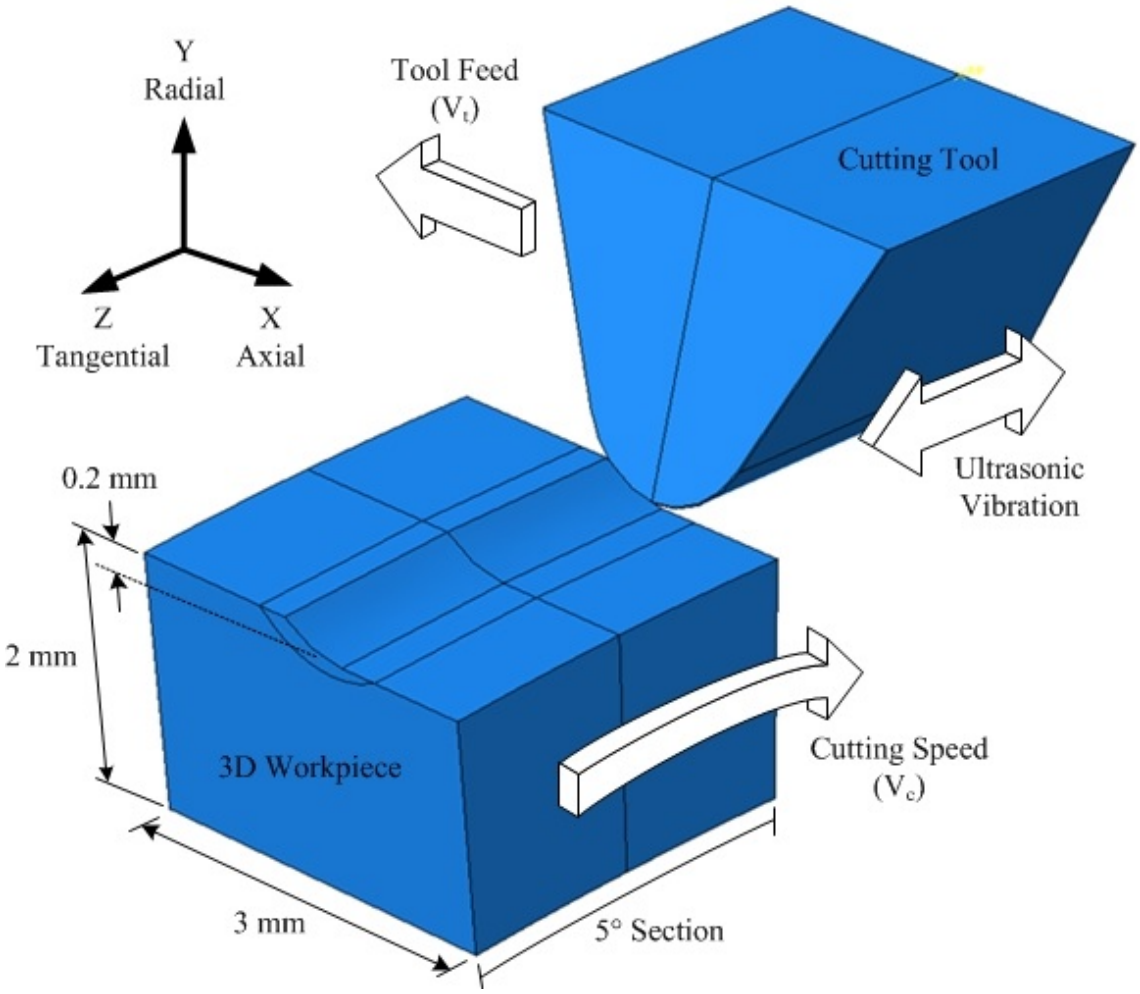

Figure 2: 3D geometry of oblique curved cutting path modelling

Table 1: 3D cutting parameters used in FE Model

Parameter	**Unit**	**Value**
Cutting speed (Surface), V_f	m/min	20
Tool feed, V_t	mm/rev	0.1
Depth of cut	mm	0.2
Ultrasonic frequency, f	Hz	20,000
Ultrasonic amplitude (peak to peak), a	µm	8

Table 2: Material parameters for Ti-6Al-4V

Material parameter	**Symbol (Unit)**	**Value**
Density	ρ (kg/m^3)	4428
Elastic modulus	E (GPa)	113.8
Poisson's ratio	ν	0.31
JC yield strength	A (MPa)	1098
JC hardening coefficient	B (MPa)	1092
JC strain hardening exponent	n	0.93
JC strain rate constant	C	0.014
JC softening exponent	m	1.1
Melting temperature	T_m (K)	1878
Transition temperature	T_g (K)	1163
JC damage constant	d_1	-0.09
JC damage constant	d_2	0.27
JC damage constant	d_3	0.48
JC damage constant	d_4	0.014
JC damage constant	d_5	3.87
Specific heat	c (J/K)	560
Heat fraction	α_0	0.9

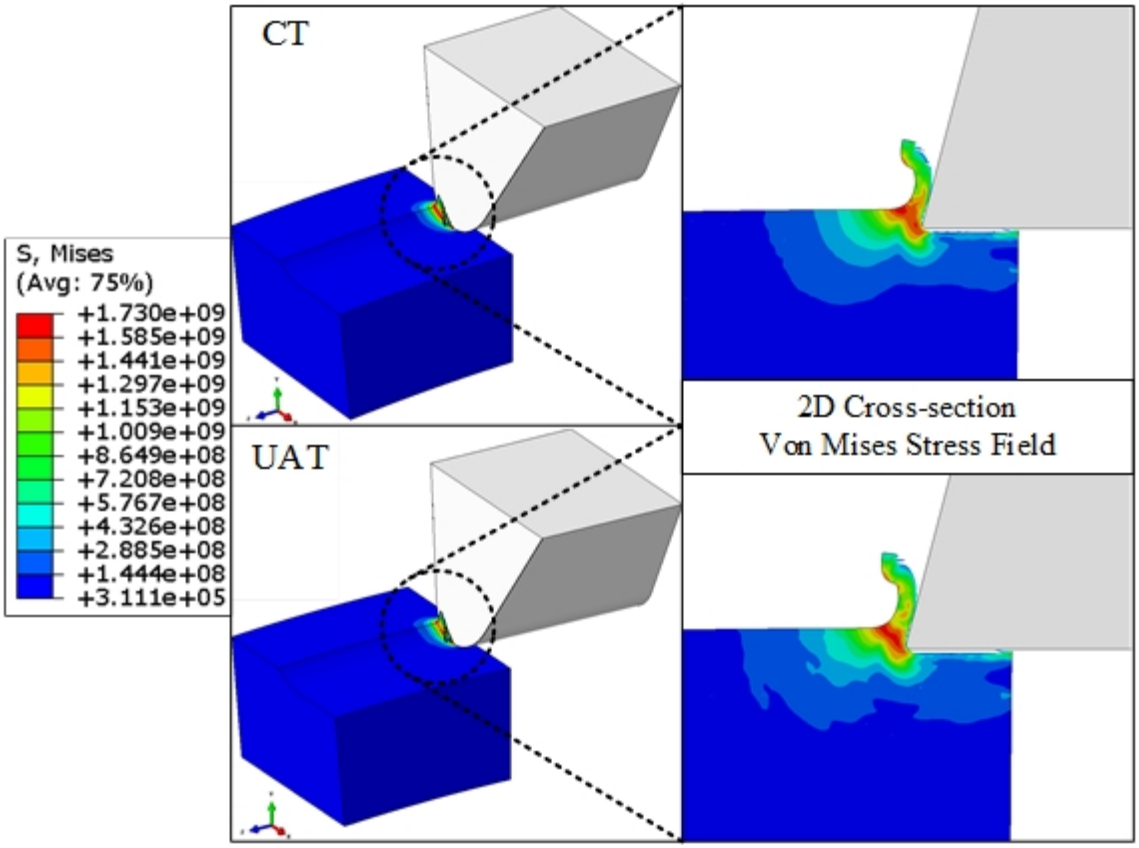

Figure 3: Comparison between von Mises stress fields within process zone for both CT and UAT